FACTA UNIVERSITATIS
Series: **Electronics and Energetics** Vol. 31, N° 1, March 2018, pp. 1 - 9
https://doi.org/10.2298/FUEE1801001E

EFFECT OF THE DISTRIBUTION OF STATES IN AMORPHOUS In-Ga-Zn-O LAYERS ON THE CONDUCTION MECHANISM OF THIN FILM TRANSISTORS ON ITS BASE

Magali Estrada[1], Yoanlys Hernandez-Barrios[1], Oana Moldovan[2], Antonio Cerdeira[1], Francois Lime[2], Marcelo Pavanello[3], Benjamin Iñiguez[2]

[1]SEES, Depto. de Ingeniería Eléctrica, CINVESTAV-IPN, México City, México
[2]Departament d'Enginyeria Electrònica, Elèctrica i Automàtica (DEEEA), Universitat Rovira i Virgili, Tarragona, Spain
[3]Department of Electrical Engineering, Centro Universitário da FEI, São Paolo, Brasil

Abstract. *Amorphous In-Ga-Zn-O Thin Film Transistors (a-IGZO TFTs) have proven to be an excellent approach for flat panel display drivers using organic light emitting diodes, due to their high mobility and stability compared to other types of TFTs. These characteristics are related to the specifics of the metal-oxygen-metal bonds, which give raise to spatially distributed s orbitals that can overlap between them. The magnitude of the overlap between s orbitals seems to be little sensitive to the presence of the distorted bonds, allowing high values of mobility, even in devices fabricated at room temperature. In this paper, we show the effect of the distribution of states in the a-IGZO layer on the main conduction mechanism of the a-IGZO TFTs, analyzing the behavior with temperature of the drain current.*

Key words: *amorphous oxide semiconductor, thin-film transistor, behavior with temperature, distribution of states*

1. INTRODUCTION

In 2004, Nomura et al. [1] presented the first amorphous oxide semiconductor (AOS) TFTs using a novel semiconductor material at that time, the amorphous In-Ga-Zn-O (a-IGZO), which was deposited by pulse layer deposition, using a KrF excimer laser and a polycrystalline In-Ga-ZnO target. The chemical composition of the target was In:Ga:Zn 1.1:1.1:0.9 in atomic ratio. The authors explained, that conduction in amorphous oxide semiconductors (AOSs) containing post-transition-metal cations is completely different

Received July 7, 2017
Corresponding author: Yoanlys Hernandez-Barrios
SEES, Depto. de Ingeniería Eléctrica, CINVESTAV-IPN, Av. IPN 2208, CP 07360, México City, México
(E-mail: yhb961210@gmail.com)

from that of covalent semiconductors as a-Si:H. In a-Si:H TFTs, the presence of randomly distributed sp_3 bonds, gives rise to a high density of both deep and tail localized states and the carrier transport is governed by hopping between localized tail states.

In AOSs, the conduction band has high ionicity due to spatially distributed s orbitals, which can overlap between them. Although distorted metal-oxygen-metal bonds exist in the amorphous material, the magnitude of the overlap between s orbitals seems to be insensitive to the presence of the distorted bonds, allowing high values of mobility, even in devices fabricated at room temperature. The transistor presented in [1] used 140-nm-thick Y_2O_3 layer as gate dielectric and Indium Tin Oxide (ITO) as source (S), drain (D) and gate (G) contacts. All materials used in the TFT were transparent.

To explain the conduction mechanism, authors previously analyzed the behavior of single-crystalline $InGaO_3(ZnO)_5$ [2]. For these devices, the carrier transport was associated to percolation conduction over potential barriers around the conduction band edge. These potential barriers are supposed to be due to randomly distributed Ga^{3+} and Zn^{2+} ions in the crystal structure. Since the amorphous IGZO (a-IGZO) TFTs showed also high mobility values with a behavior similar to the crystalline ones, authors considered that the percolation conduction mechanism takes place also in a-IGZO TFTs [3].

Due to the relatively high electron mobility, high optical transparency, low temperature and relatively low cost processing techniques, these devices have found an important application in Active Matrix Organic Light Emitting Diodes, (AMOLEDs) displays [4-7].

From this moment on, a-IGZO TFTs have been object of continuous and intensive research from all points of view, including technological and physical aspects, looking to improve stability, increase mobility and reduce operating voltage range, among others.

The characteristics of the a-IGZO band structure can be found in [6,7], with a distribution of bulk localized states DOS in the gap [7,8]. It is generally accepted that DOS observed in a-IGZO layers are characterized by a relatively low density of localized states, less than $1x10^{20}$ $cm^{-3}eV^{-1}$, and their characteristics strongly depend on the process used for the IGZO layer deposition and in general on the device fabrication [9-13].

Regarding the conduction mechanism, in [14], authors proposed a conduction mechanism that contains both possibilities, band percolation [15] and the mobility edge or multiple trapping and release mechanism [16,17], which they call extended mobility edge model. Depending on the specific characteristics of the device associated to the fabrication process, or depending on the operation regime for the same device, the predominant mechanism can be either percolation in conduction band or multiple trapping.

The characterization with temperature of the electrical characteristics of TFTs allows to analyze, not only the behavior of the devices in the temperature operation range required for the specific application, but also the conduction mechanisms. In most amorphous TFTs, the drain current has been reported to increase with temperature, which is characteristic of the hopping conduction mechanism.

In this paper, we show, that under certain operation conditions, a reduction of the drain current with temperature is observed, which is related to the characteristics of the DOS present in the a-IGZO layer of the device.

2. EXPERIMENTAL PART

For the analysis of the electrical characteristics, we will use two bottom gate top contact IGZO TFTs shown in Figures 1a and b. Device 1 consists of 90 nm of HfO_2 as gate dielectric, deposited at 100 ^oC by atomic layer deposition, on top of which, a 70 nm thick IGZO layer was deposited by pulsed laser deposition (PLD) at 20 mTorr oxygen pressure. A 500 nm thick layer of poly-p-xylylene-C (Parylene-C), deposited by chemical vapor deposition (CVD) at room temperature at 1 mTorr, was used as etch stopper layer (ESL). Au/Cr deposited by electron beam was used for gate contact and Al was used for drain and source contacts. Annealing was done after the deposition of the a-IGZO layer and at the end of the fabrication process.

Device 2 consisted of 200 nm of Si_3O_4 as gate insulator, deposited by Plasma Enhanced Chemical Vapor Deposition (PECVD), at 250 ^oC as gate insulator. The a-IGZO layer had 12 nm and was deposited by RF sputtering at room temperature. As etch stopper layer, 100 nm of SiO_2, deposited by PECVD, were used. Mo/Cr was used for *G*, *D* and *S* contacts. A final annealing was done at the end of the fabrication process. Photolithography was used to pattern each layer. Figures 1a and b show the cross section of Device 1 and 2, respectively.

The analyzed TFTs corresponding to Device 1 had channel width (*W*) and length (*L*) of *W*=80 µm *L*=40 µm and those of Device 2 had *W*=900 µm, *L*=30 µm.

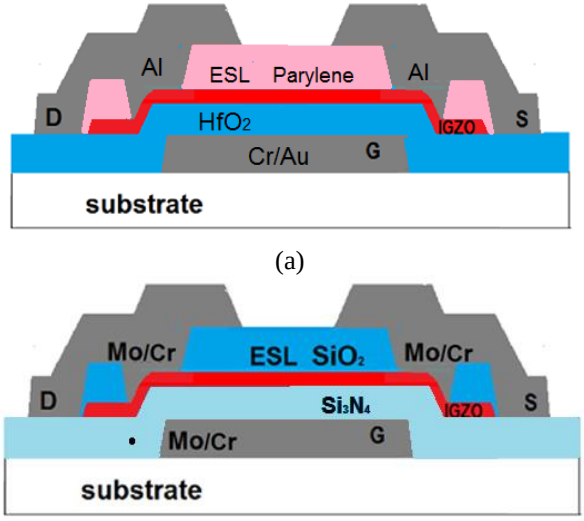

Fig. 1 a) Cross section of IGZO TFT referred as: a) Device 1; b) Device 2.

Electrical measurements were done at different temperatures and in vacuum conditions, using a K20 programmable Temperature Controller and measurement chamber from MMR Technologies Inc. and a Keithley 4200 semiconductor characterization system.

The output characteristics were measured every ten degrees, in the temperature range between 300 K and 350 K. Measurements were done after waiting 5 minutes at each fixed temperature, with no applied bias. The time with applied voltage, during measurements at

each temperature, was less than 5 min. Before the I-V-T measurements, the devices were tested for hysteresis and bias stress instability at room temperature to guarantee that the variation of the drain current was due to the temperature variation and not to instability effects.

3. ANALYSIS AND DISCUSSION

Figure 2a shows the measured output characteristics at 300, 320 and 330 K for Device 1. Fig. 2b shows the output characteristics at 300,330 and 350 K for Device 2. As can be seen in Fig. 2a, the drain current (I_{DS}) increases significantly with temperature. This is the typical behavior with temperature of the output current in a-IGZO shown in [12,14,17,18,19]. On the contrary, in the output characteristics shown in Fig. 2b, I_{ds} reduces with the increase of T, as V_{DS} increases.

As already mentioned, due to the specific characteristics of metal oxide materials chemical bonds, the conduction mechanism in a-IGZO TFTs can be due not only to hopping, typical of amorphous TFTs, but also to percolation in the conduction band [8,9,14]. The temperature dependence of the drain current and mobility will be determined by the predominant conduction mechanism, which can depend, not only on the fabrication process, but on the operation conditions for a given fabrication process.

It is expected that the contribution of the Variable Range Hopping (VRH) becomes greater than the band-like mechanism when the Fermi level E_F lies within the exponential tail states. According to [14], for a characteristic energy of around kT_a=0.069 eV and a density of acceptor tail states at E_c, (N_{ta}) in the order of $3.4\text{x}10^{19}$ $\text{cm}^{-3}\text{eV}^{-1}$, this can occur.

To estimate the DOS in the amorphous semiconductor material of our devices, we used the same procedure as in [16,17], obtaining characteristic energy of kT_a =0.072 eV and N_{ta} = $8.5\text{x}10^{19}$ $\text{cm}^{-3}\text{eV}^{-1}$ for Device 1 and kT_a=40 meV and N_{ta}<$6\text{x}10^{18}$ $\text{cm}^{-3}\text{eV}^{-1}$ for Device 2.

In order to study in more detail the effect of the DOS characteristic on the conduction mechanism, we used simulations in ATLAS. For this purpose, we simulated the output characteristics for a-IGZO TFTs with a bottom gate structure.

Different DOS characteristics with an acceptor-type DOS, having N_{ta} values in the range from $1.5\text{x}10^{20}$ $\text{cm}^{-3}\text{eV}^{-1}$to $3.5\text{x}10^{17}$ $\text{cm}^{-3}\text{eV}^{-1}$ were simulated. The characteristic energy was varied from 0.03 eV to 0.18 eV. The default low field mobility model was used, taking the default value of the temperature dependent parameter for this mobility in ALTAS. The reduction of mobility with temperature is the typical behavior expected for a crystalline device due to phonon scattering. In this case, it can be associated to a crystalline-like behavior of the amorphous oxide semiconductor material [3].

The mobility dependence with temperature is considered with the objective to distinguish between the effect of the characteristics of the DOS and the effect of a crystalline-like mobility behavior, on the I_{DS} temperature dependence. If mobility is considered constant in the simulator, the variation of the drain current with temperature will be determined only by the DOS characteristics, which was confirmed by simulating considering a mobility that does not depend on temperature. The model used for the Blaze simulation included Fermi statistics, as well as band parameters and bandgap narrowing specified for IGZO material.

Main results of simulations are summarized on Table I. For simulated output characteristics of devices with N_{ta}=1.5x10^{20} cm^{-3}eV^{-1} and kT_a=0.34, the typical increase of I_{DS} with T was observed for all curves with V_{GS} equal or above 4 V. It is evident that in this case, defects are determining the behavior of the temperature dependence of the drain current.

For values of N_{ta} equal or below 1.5x10^{19} cm^{-3}eV^{-1}and kT_a=0.034 eV, the drain current decreases with temperature. This result confirms that when, the density of localized states is sufficiently small and trapping is less important, the temperature dependence of the drain current is determined by the temperature dependence of mobility, see Table 1.

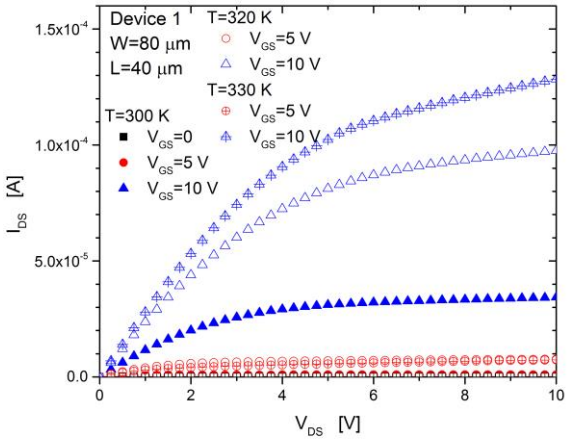

(a)

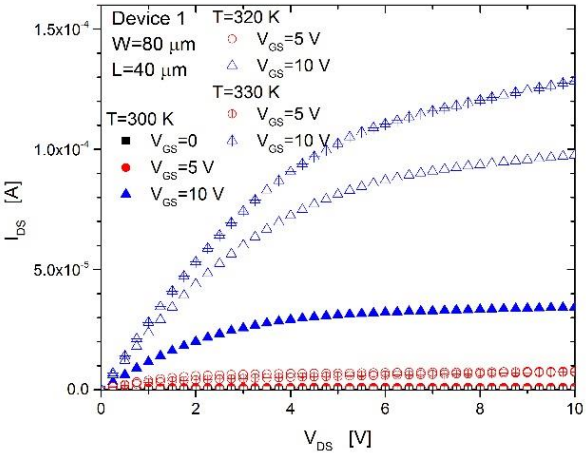

(b)

Fig. 2 Output characteristics at different temperatures, of: a) Device 1; b) Device 2´.

The effect of reducing the DOS characteristic energy kT_a, and thus the effect of trapping, was also analyzed. For this purpose N_{ta} was maintained constant and equal to N_{ta}=3.5x10^{19} cm^{-3}eV^{-1}, while the characteristic energy was varied. Table 1 and Fig. 3 show that the reduction of kT_a allows the change of mechanism to occur for smaller values of V_{GS}. It is observed that for kT_a=100 meV, the change in mechanism is not observed and I_{DS} at 350 K is higher than at 300 K for all the operation voltage range. For kT_a =70 meV, the change in mechanism is observed only, for V_{GS}=10 V, when I_{DS} at 350 K becomes smaller than at 300 K. For kT_a =0.34, the conduction mechanism is also the same in all the operation voltage range, but it corresponds to percolation in the conduction band, producing the reduction of I_{DS} with T. Fig. 4 shows the change of mechanism in a simulated transfer curve in saturation, when N_{ta} is changed maintaining kT_a =0.034 eV. For N_{ta} = 1.5x10^{20} cm^{-3}eV^{-1}, I_{DS} is higher at 350 K than at 300 K for all values of V_{GS}. For N_{ta} =1.5x10^{18} cm^{-3}sV^{-1}, I_{DS} is practically the same at 300 and 350 K for V_{DS}<-0.5 V and as V_{GS} increases, the drain current at 350 K becomes smaller than at 300 K.

Table 1 Values of the drain current for T=300 K and 350 K, at V_{DS}=10 V and different values of V_{GS}, corresponding to different combinations of values of N_{ta} and kT_a.

N_{ta} (cm^{-3})	kT_a (meV)	I_{DS} [A] V_{DS}=10 V V_{GS}=4 V T=350 K T=300 K	I_{DS} [A] V_{DS}=10 V V_{GS}=6 V T=350 K T=300 K	I_{DS} [A] V_{DS}=10 V V_{GS}=8 V T=350 K T=300 K	I_{DS} [A] V_{DS}=10 V V_{GS}=10 V T=350 K T=300 K
1.5x10^{18}	34	2.05x10^{-5} 2.54x10^{-5}	4.00x10^{-5} 4.98x10^{-5}	6.58x10^{-5} 8.23x10^{-5}	9.65x10^{-5} 1.21x10^{-4}
1.5x10^{19}	34	1.64x10^{-5} 1.89x10^{-5}	3.30x10^{-5} 3.89x10^{-5}	5.57x10^{-5} 6.66x10^{-5}	8.34x10^{-5} 1.01 x10^{-4}
1.5x10^{20}	34	4.06 x10^{-6} 3.20 x10^{-6}	9.13 x10^{-6} 7.83 x10^{-6}	1.71 x10^{-5} 1.50 x10^{-5}	2.85x10^{-5} 2.80 x10^{-4}
1.5x10^{19}	100	2.09 x10^{-6} 1.50 x10^{-6}	7.36 x10^{-6} 6.68 x10^{-6}	1.74 x10^{-5} 1.78 x10^{-5}	3.29x10^{-5} 3.59x10^{-5}
3.5x10^{19}	34	1.22 x10^{-5} 1.83 x10^{-5}	2.56 x10^{-5} 3.69 x10^{-5}	4.44 x10^{-5} 6.19 x10^{-5}	6.83x10^{-5} 9.21x10^{-5}
3.5x10^{19}	70	2.13 x10^{-6} 1.44 x10^{-6}	6.51 x10^{-6} 5.41 x10^{-6}	1.48 x10^{-5} 1.40 x10^{-5}	2.77 x10^{-5} 2.85 x10^{-5}
3.5x10^{19}	100	2.10 x10^{-7} 8.80 x10^{-7}	1.08 x10^{-6} 6.36 x10^{-7}	3.69 x10^{-6} 2.83 x10^{-6}	9.38 x10^{-6} 8.55 x10^{-6}
6x10^{19}	30	1.07 x10^{-5} 1.08 x10^{-5}	2.24 x10^{-5} 2.37 x10^{-5}	3.92 x10^{-5} 4.31 x10^{-5}	6.08 x10^{-5} 6.87 x10^{-5}
8.5x10^{19}	72	2.84 x10^{-7} 1.25 x10^{-7}	1.03 x10^{-6} 5.78 x10^{-7}	2.85 x10^{-6} 1.95 x10^{-6}	6.53 x10^{-6} 5.22 x10^{-6}
3.5x10^{17}	180	1.83 x10^{-5} 2.25 x10^{-5}	3.69 x10^{-5} 4.58 x10^{-5}	6.19 x10^{-5} 7.72 x10^{-5}	9.21 x10^{-5} 1.15 x10^{-4}

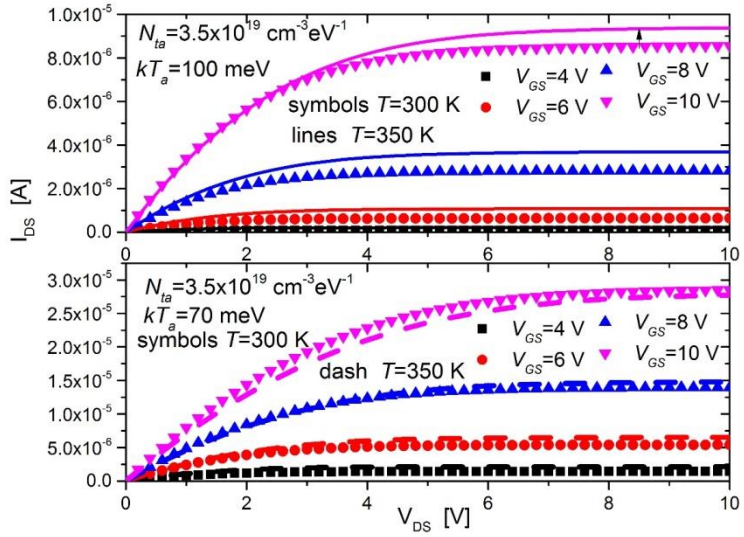

Fig. 3 Simulated output characteristics at T=300 K and T=350 K for N_{ta}= 3.5x10^{19} cm^{-3}eV^{-1} and kT_a=100 meV and 70 meV, showing the different behavior of I_{DS} with T corresponding to the change in conduction mechanism.

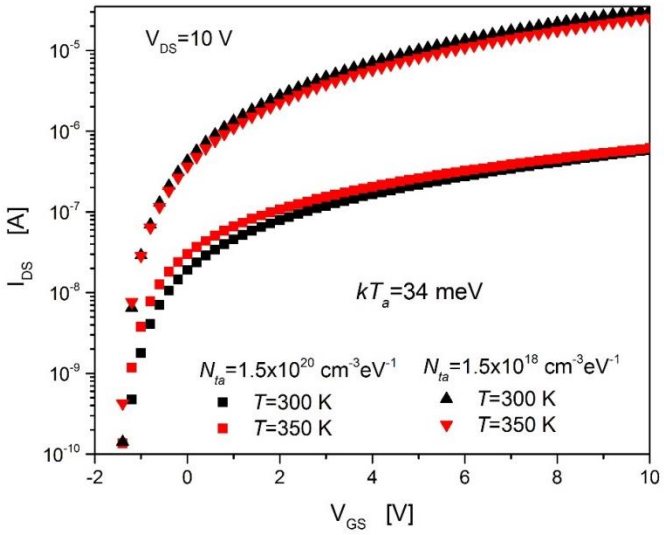

Fig. 4 Simulated transfer curves in saturation at T=300 K and T=350 K for N_{ta}= 1.5x10^{20} cm^{-3}eV^{-1} and 1.5x10^{18} cm^{-3}eV^{-1}, for kT_a =34 meV.

Simulations confirm that Device 1 with the DOS characteristic indicated above, is expected to have hopping as the predominant conduction mechanism in all the operation region and temperature range analyzed, which is what was observed.

From the other hand, simulations also show that for values of N_{ta} below $3.5x10^{19}$ cm^{-3} and kT_a below 0.1 eV, the predominant conduction mechanism can change to percolation for V_{DS} and V_{GS} above a given value. This value can be estimated analyzing the Arrhenius dependence of the drain current in the devices. This was the case observed for Device 2.

As already mentioned, the presence of bandlike carrier transport is well accepted for IGZO TFTs, although the presence of VRH cannot be excluded [14]. Due to it, the device can reveal an electrical crystalline-like behavior, in which mobility reduces with temperature, due to the interaction of carriers with the atoms in the material. The predominant carrier transport mechanism, will depend on the DOS characteristics of the device being analyzed. If the effect of the DOS, is sufficiently small, the current due to percolation conduction is expected to become predominant and the device can show a crystalline-like behavior.

4. CONCLUSIONS

Due to the chemical bond of in a-IGZO layers, carrier conduction in the conduction band is possible in AOSTFTs based on this material. However, the presence of VRH cannot be excluded and the predominant conduction mechanism is determined by the characteristics of the DOS in the amorphous IGZO layer and the operating voltages, which will define the position of the Fermi level.

Simulations confirm that, when the effect of the DOS, is sufficiently small, that is when the combination of N_{ta} and kT_a is sufficiently small, current due to percolation conduction becomes predominant and the device can show a crystalline-like behavior in the operation range. For example, for a density of tail acceptor states N_{ta}=$3.5x10^{19}$ $cm^{-3}eV^{-1}$ and a characteristic energy of 34 meV, I_{DS} reduces with T. For kT_a=100 meV the current increases with T. For kT_a =70 meV, the drain current decreases only when V_{GS}=10 V. For N_{ta} =$1x10^{20}$ $cm^{-3}eV^{-1}$ the current increases with T even for kT_a =34 meV, indicating that VHR conduction is predominant. For N_{ta} <$1.5e^{19}$ $cm^{-3}eV^{-1}$, the current reduces with T for kT_a =34 meV, indicating that the percolation conduction mechanism is predominant in all the operating voltage range of the TFT.

Acknolwledgement: *This work was supported by CONACyT projects 237213 and 236887 in Mexico, the H2020 programme of the European Union under contract 645760 (DOMINO), by contract "Thin Oxide TFT SPICE Model" (T12129S) with Silvaco Inc., by ICREA Academia 2013 from ICREA Institute and the Spanish Ministry of Economy and Competitiveness through project TEC2015-67883-R (GREENSENSE). The authors acknowledge Holst Centre/TNO and Dr. I. Mejia, from the University of Texas at Dallas, for providing the TFT devices.*

REFERENCES

[1] K. Nomura, H. Ohta, A. Takagi, T. Kamiya, M. Hirano, H. Hosono, "Room-temperature fabrication of transparent flexible thin-film transistors using amorphous oxide semiconductors", *Nature,* vol. 432, pp. 488-492, 2004.

[2] K. Nomura, T. Kamiya, H. Ohta, K. Ueda, M. Hirano, H. Hosono. "Carrier transport in transparent oxide semiconductor with intrinsic structural randomness probed using single-crystalline InGaO3(ZnO)5 films", *Appl. Phys. Lett.,* vol. 85, pp. 1993-1995, 2004.

[3] T. Kamiya, K. Nomura, H. Hosono, "Electronic Structures Above Mobility Edges in Crystalline and Amorphous In-Ga-Zn-O: Percolation Conduction Examined by Analytical Model", *J. Display Technol.,* vol. 5, pp. 462-467, 2009.

[4] E. Fortunato, P. Barquinha, R. Martins, "Oxide semiconductor thin-film transistors: A review of recent advances", *Adv. Mater.,* vol. 24, pp. 2945-2986, 2012.

[5] H. Kumomi, T. Kamiya, H. Hosono, "Advances in Oxide Thin-Film Transistors in Recent Decade and Their Future", *ECS Transactions,* vol. 67, pp. 3-8, 2015.

[6] T. Kamiya, H. Hosono, "Material characteristics and applications of transparent amorphous oxide semiconductors", *NPG Asia Mater.,* vol. 2, pp. 15-22, 2010.

[7] T. Kamiya, K. Nomura, H. Hosono, "Present status of amorphous In-Ga-Zn-O thin-film transistors", *Sci. Technol. Adv. Mater.,* vol. 11, pp. 044-305.

[8] T. Kamiya, K. Nomura, H. Hosono, "Electronic structure of the amorphous oxide semiconductor a-InGaZnO4–*x:* Tauc–Lorentz optical model and origins of subgap states", *Phys. Status Solidi A,* vol. 206, pp. 860–867, 2009.

[9] S. Sallis, K.T. Butler, N.F. Quackenbush, D.S. Williams, M. Junda, D.A. Fischer, J.C. Woicik, N.J. Podraza, B.E. White, A. Walsh, L.F. Piper, "Origin of deep subgap states in amorphous indium gallium zinc oxide: Chemically disordered coordination of oxygen", *Applied Physics Letters,* vol. 104, pp. 232108, 2014.

[10] S. C. Kim, Y.S. Kim, J. Kanicki, "Density of states of short channel amorphous In–Ga–Zn–O thin-film transistor arrays fabricated using manufacturable processes", *Jpn. J. of Appl. Phys.,* vol. 54, pp. 51-101, 2015.

[11] X. Ding, J. Zhang, W. Shi, H. Zhang, C. Huang, J. Li, X. Jiang, Z. Zhang, "Extraction of density-of-states in amorphous InGaZnO thin-film transistors from temperature stress studies", *Current Applied Physics,* vol. 14, pp. 1713-1717, 2014.

[12] C. Chen, K. Abe, H. Kumomi, J. Kanicki, "Density of states in a-InGaZnO from temperature dependent field studies", *IEEE Tran. Electron Devices,* vol. 56, pp. 1177-1183, 2009.

[13] J. Jeong, J.K. Jeong, J.S. Park, Y.G. Mo, Y. Hong, "Meyer–Neldel Rule and Extraction of Density of States in Amorphous Indium–Gallium–Zinc-Oxide Thin-Film Transistor by Considering Surface Band Bending", *Japanese Journal of Applied Physics,* vol. 49, pp. 03CB02, 2010.

[14] W. Chr. Germs, W.H. Adriaans, A.K. Tripathi, W.S.C. Roelofs, B. Cobb, R.A. J. Janssen, G.H. Gelinck, M. Kemerink, "Charge transport in amorphous InGaZnO thin-film transistors", *Phys. Rev.,* vol. B86, pp. 155-319, 2012.

[15] T. Kamiya, K. Nomura, H. Hosono, "Origin of definite Hall voltage and positive slope in mobility-donor density relation in disordered oxide semiconductors", *Appl. Phys. Lett.,* vol. 96, pp. 122103, 2010.

[16] S. Lee, S. Park, S. Kim, Y. Jeon, K. Jeon, J.-H. Park, J. Park, I. Song C., J. Kim, Y. Park, D.M. Kim, D.H. Kim, "Extraction of Subgap Density of States in Amorphous InGaZnO Thin-Film Transistors by Using Multifrequency Capacitance–Voltage Characteristics", *IEEE Electron Device Lett.,* vol. 31, pp. 231-233, 2010.

[17] J.-H. Park, K. Jeon, S. Lee, S. Kim, S. Kim, I. Song, J. Park, Y. Park, C. J. Kim, D. M. Kim, D.H. Kim, "Self-Consistent Technique for Extracting Density of States in Amorphous InGaZnO Thin Film Transistors", *J. Electrochem. Soc.,* vol. 157, pp. H272, 2010.

[18] P.Y. Liao, T.C. Chang, T.Y. Hsieh, M.Y. Tsai, B.W. Chen, Y. H. Tu, A. K. Chu, C.H. Chou, J.F. Chang, J F "Investigation of carrier transport behavior in amorphous indium–gallium–zinc oxide thin film transistors", *Jpn. J. of Appl. Phys.,* vol. 54, pp. 094101, 2015.

[19] M. Estrada, M. Rivas, I. Garduño, F. Avila-Herrera, A. Cerdeira, M. Pavanello, I. Mejia, M.A. Quevedo-Lopez, "Temperature dependence of the electrical characteristics up to 370 K of amorphous In-Ga-ZnO thin film transistors", *Microelectronics Reliability,* vol. 56, pp. 29–33, 2016.